Preparation and characterization of tin (II) oxide powder as *p*-type semiconductor for its deposition by ink jet printing

Author: Jorge Carlos Vergara Cruz.
Facultat de Física, Universitat de Barcelona, Diagonal 645, 08028 Barcelona, Spain.

Abstract: The synthesis through a simple chemical route of SnO powder was successfully done. By using a home-made Hall-effect setup, its p-type behaviour is confirmed, showing high hole mobility around 10^2 $cm^2 \cdot V^{-1} \cdot s^{-1}$ and low resistivity ρ=6.52 Ω·m. Moreover the powder exhibits an interesting behaviour with the temperature changing its conformation to SnO_2 that is *n*-type semiconductor.

I. INTRODUCTION

Nowadays oxide semiconductors are widely investigated, due to their optical and electrical properties, for gas sensors, solar cells or TFT devices. Most of these semiconductors are *n*-type with high electron mobility and the challenge is to achieve *p*-type semiconductor, without doping particles in order to ensure a high hole mobility. There are few reports about this subject, but the trend techniques use physical depositions like sputtering [1], [2], nanowire fabrication [3] to obtain doped *n*-type semiconductors. The greatest difficulty is to obtain a *p*-type semiconductor by chemical fabrication and the creation of a stable ink from the resultant powder.

Naturally *p*-type tin oxide (SnO) exhibits a huge range of hole mobilities from 0.02 $cm^2 \cdot V^{-1} \cdot s^{-1}$ to 131 $cm^2 \cdot V^{-1} \cdot s^{-1}$, for thin film configuration, and carrier concentrations from $3.29 \cdot 10^{13}$ cm^{-3} to $1.47 \cdot 10^{19}$ cm^{-3} respectively [1]. Moreover, *p*-type doped SnO_2 films shows lower mobility [4], supporting the statement of not doped-SnO *p*-type films are needed to achieve the transistor effect with a high mobility of the carriers.

The inkjet technique exhibits some advantages over physical deposition techniques. For example inkjet printers can fabricate, in short time, complex circuits and flexible substrates can be used.

In this *TFG* I was encouraged to:

1. Synthesize and analyse of SnO powder.
2. Deposit it via drop coating and spin coating.
3. Measure the electrical properties of the thin films

Moreover to do the electrical measurements I created a prototype setup in which the resistivity, the doping type, the sheet carrier density and the mobility of the majority carriers could be measure using the van der Pauw method.

II. EXPERIMENTAL

To synthesize the SnO powder a simple chemical route of acid-base reactions was used. First of all 5 g of $SnCl_2 \cdot 2H_2O$ where diluted in 2 ml of concentrated HCl. Then it was reduced with a saturated NaOH solution till reach pH 9. This solution was heated at 70ºC for 45 minutes on a hot plate, after that a black powder precipitated and, in order to clean the precipitate, I siphoned it with hot-distilled water until only remains the powder (SnO). Finally I recovered the precipitate using a Kitasato and a Buchner funnel. After that the powder was dried on a hot plate at 80ºC for 45 minutes.

To produce the dissolution four different dissolvents were used. In one hand, water, ethanol and acetone were used to do the drop coating method, a little quantity of the powder was mixed with these dissolvents and deposited using a syringe on a glass substrate. In the other hand, 30 ml of ethylene glycol was mixed with 0.1 g of SnO powder and kept in an ultrasound bath for 45 minutes. A small quantity of the dissolution was dropped on the glass substrate and spined for 1 min at 310 rpm. With the exceeding powder two discs of 0.9 mm of thickness where created.

The electrical properties and Hall coefficients were measured with the van der Pauw method using a four contacts system and magnetic fields, for the Hall's effect, of 15 G, 25 G and 35 G.

III. RESULTS AND DISCUSSION

A. POWDER

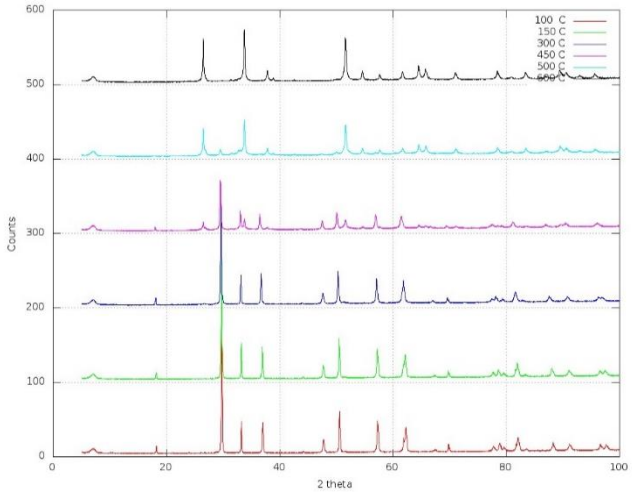

FIG.1: XRD of SnO Powder and its variation with temperature from botton to top the temperatures are 100, 150, 300, 450 500 and 600 ºC**.**

X-ray diffraction (XRD, Fig. 1) and thermal (Fig. 2) analyses of the SnO powder were performed. In Fig. (1) we can see a change of crystallinity with the temperature due to the transition from SnO to SnO_2. To confirm what happened, simultaneous Differential ThermoGravimetry (DTGA), Differential thermal analysis (DTA) and Differential scanning calorimetry (DSC) tests were performed to measure mass, temperature and heat evolutions respectively while adding energy. At the temperature of 425ºC the SnO starts an oxidation process to SnO_2 because TGA shows an intense peak at 576ºC. The DSC and DTA confirm that the mass variation

is due to an oxidation because the curves are maxima. Moreover, we can calculate the molar variation of the process on the hypothesis that the initial mass is all SnO (molar mass of 134.71 g/mol) and the final mass is all SnO_2 (molar mass of 150.71 g/mol). So, if our supposition is right the molar variation will be 0%. The initial mass was of 17.63 mg and the final was 19.46 mg giving a molar loss of 1.5%. This small discrepancy is due to an uncertainty on the initial mass because of the evaporation of substances that are not SnO and the process before reaching the initial temperature.

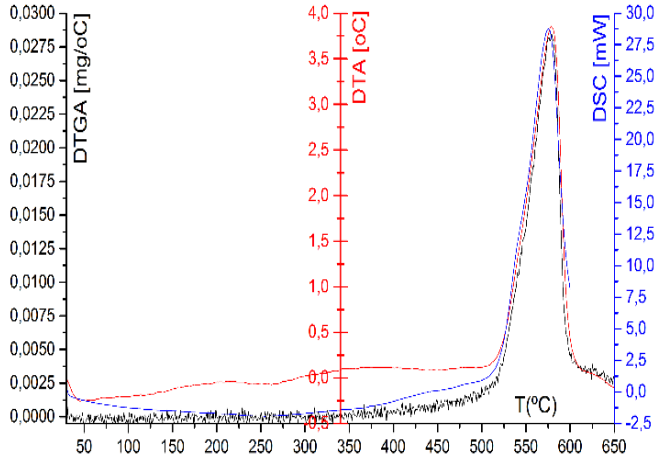

FIG.2: DTGA+DSC+DTA results.

There exist several reports about the crystalline shape of the SnO nanocrystals [5] and because of the inkjet printers accept a maximum of grain size below one micrometre, we need to know the size and shape of our crystals. To do so the powder was analysed with Scanning Electron Microscopy (SEM). Basically we observed two different forms of crystals. The flower-like crystal of Fig. (3), similar to the obtained by [6], they are about 20 μm large. The other structure is a square-like crystal about 20 μm side, but someone are smaller Fig. (4). In [6] authors suggest that the flower-like is a superposition of several squares.

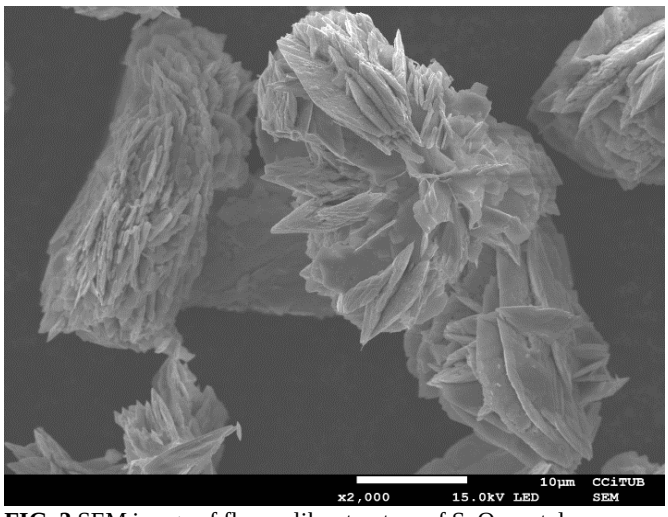

FIG. 3 SEM image of flower-like structure of SnO crystal.

B. DISSOLTION AND DEPOSITION

SnO is amphoteric, needs acid or a basic medium to be dissolved [7], and the last one is the case of ethylene glycol. An intuitive idea get us to a simple reduction reaction, where stannites are formed, but it is not clear at all that the ion Sn^{2+} has preference over ion Sn^{4+}. If the second ion is formed, the film produced with that solution will be of SnO_2 and the goal will not be achieved. Only a little part of the powder was dissolved in ethylene glycol but shaking the solution, the powder can be kept in suspension for a short time, enough to do the coat. The film created so has the particles too separated and do not show percolation path for electricity. Similar results were obtained with water, ethanol and acetone, and no film produced was useful to do the electrical measurements. This is the reason because I decided to fabricate the powder compressed disks. The deposition by inkjet must also be disregarded.

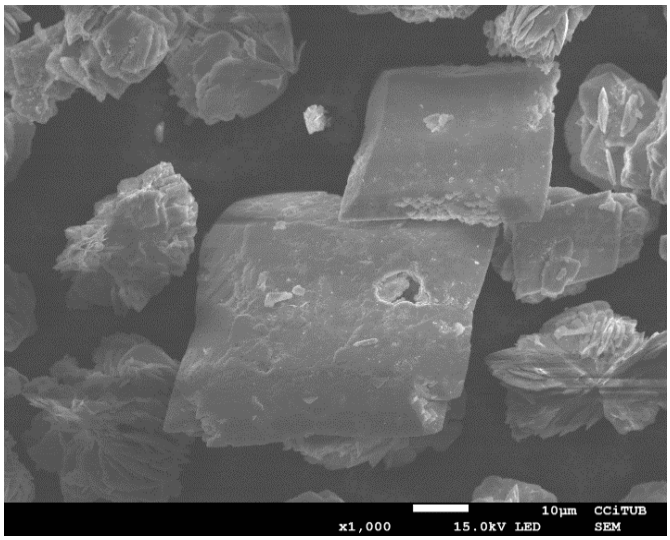

FIG 4. SEM image of square-like structure of SnO.

C. ELECTRICAL CHARACTERIZATION

In order to verify the precision of the home-made Hall-effect device, a previous measurement of the electrical properties of known thin films was performed. In table (1) the results and the reference values are shown.

	ρ (Ω·m)	ρ' (Ω·m)	n (cm^{-3})	n' (cm^{-3})
IS73	$5.45\cdot10^{-6}$	$5.74\cdot10^{-6}$	$3.80\cdot10^{20}$	$3.69\cdot10^{20}$
IS69	$2.05\cdot10^{-1}$	$1.3\cdot10^{-1}$	$1.49\cdot10^{18}$	$8.07\cdot10^{17}$

TABLE 1. Resistity and carrier concetration comparation between calculated (ρ, n) and real values (ρ',n') for the test films.

In the van der Pauw method four ohmic contacts are placed in the edges of the surface, they are labelled from 1 to 4 in counter-clockwise order Fig. (5). $R_{12,34}$ is the Ohm relation between the current injected from contact 1 to contact 2 (I_{12}) and the DC voltage between contact 3 and 4 with no magnetic field applied (V_{34}). Following the same logic the other resistances are calculated. The R_H and R_V are calculated as the mean resistances of the currents injected in the horizontal and vertical directions respectively, in both direct and reverse polarities are used in order to improve the accuracy of the values removing offset voltages.

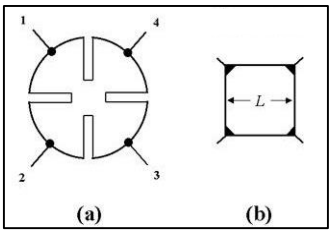

FIG.5 The two geometries chosen for the experiments

To calculate the sheet resistance of the surface, Rs, we solved the van der Pauw equation (1) by numerical methods:

$$e^{-\frac{\pi R_H}{R_S}} + e^{-\frac{\pi R_V}{R_S}} = 1 \qquad (1)$$

Finally multiplying R_S with the thickness of the film we can calculate the resistivity of the film.

$$\rho = R_s * t \qquad (2)$$

Moreover if we know the carrier concentration n, we could calculate the mobility of the majoritarian carriers thanks to formula (3).

$$\mu = \frac{1}{q\rho n} \qquad (3)$$

To know the carrier concentration and the nature of the semiconductor, the Hall's effect was used. The Hall's voltage was always measured by using the same intensity, but depending of the surface to analyse. Moreover, different magnitudes and directions of magnetic fields were used to improve the carrier concentration determination and, as in the resistance calculation, reverse and direct polarities have been considered. The final calculation of the Hall's tension, V_H, is obtained with:

$$\begin{aligned} V_{13} &= V_{13,P} - V_{13,N} \\ V_{24} &= V_{24,P} - V_{24,N} \\ V_{31} &= V_{31,P} - V_{31,N} \\ V_{42} &= V_{42,P} - V_{42,N} \end{aligned} \qquad (4)$$

$$V_H = \frac{V_{13} + V_{24} + V_{31} + V_{42}}{8} \qquad (5)$$

In equation (4) the subscripts P and N are referred to positive and negative magnetic fields respectively, where the positive is a magnetic field that enters the surface and negative is an out-coming magnetic field. The numerical subscripts indicate the contacts where the voltage was measured and in the case of $V_{24(13)}$ the intensity was $I_{13(24)}$ and in the case of $V_{42(31)}$ the intensity was $I_{31(24)}$. As we said before, this is for the minimization of the uncertainty in the Hall's Voltage. Fig. (6), shows the relation between, for Disk 1, Hall's voltage and magnetic field magnitude measured by using this procedure.

These results are ambiguous. In one hand, the carrier concentration can not be exactly determined due to the high dispersion of the measure. Notwithstanding, all the measured voltages are greater than zero and so the majoritarian carriers are holes. Moreover the magnitude order of the carrier concentration can be settled approximately between 10^{11} and 10^{12} cm^{-3} thanks to formula (6). These values are similar to those of conventional semiconductors like silicon or gallium arsenide.

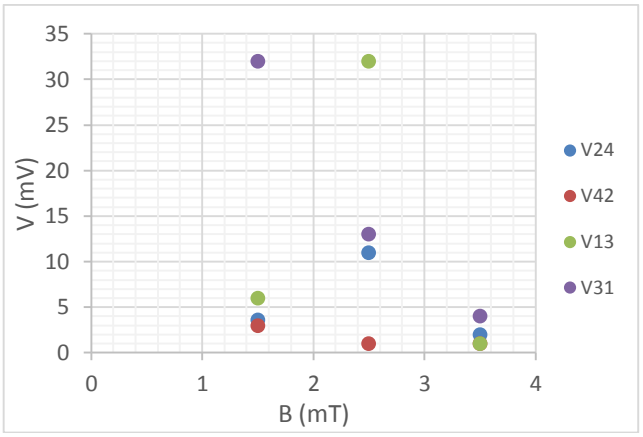

FIG. 6 Hall's effect with constant intensity of 85 μA in SnO disc, red points are V_{13} and the blue ones are V_{24}.

$$V_H = \frac{IB}{qnt} \qquad (6)$$

In the other hand the resistivity measure is good enough. The results of two of the four measures are represented in Fig.(7) and Fig. (8).

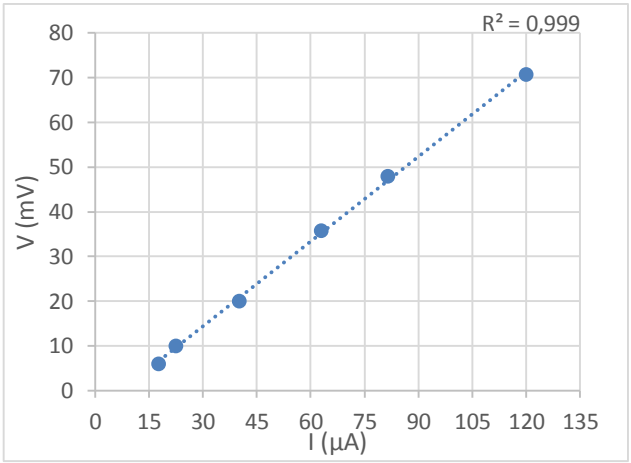

FIG .7 V(I) of SnO disc 1, the slope is the resistance $R_{23,14}$=632 Ω.

In these graphics a clearly ohmic behaviour is visible, and using the equations (1) and (2), R_s and then the resistivity could be determined thanks to the formula relating Resistance with resistivity (7).

$$\rho = R\frac{S}{l} = R_s * t \qquad (7)$$

The result is ρ = 6.52 Ωm, very similar to the intrinsic GaAs value (ρ ≈ 5 Ωm). Furthermore, there exists a clearly asymmetry in the contacts due to their size that it is too much big in relation to the dimensions of the SnO disc. This could also be the reason of the huge dispersion in the Hall measurement.

Once the resistivity and the carrier concetration are known it is easy to calculate the mobility by the equation (3) where q is the elemental charge.

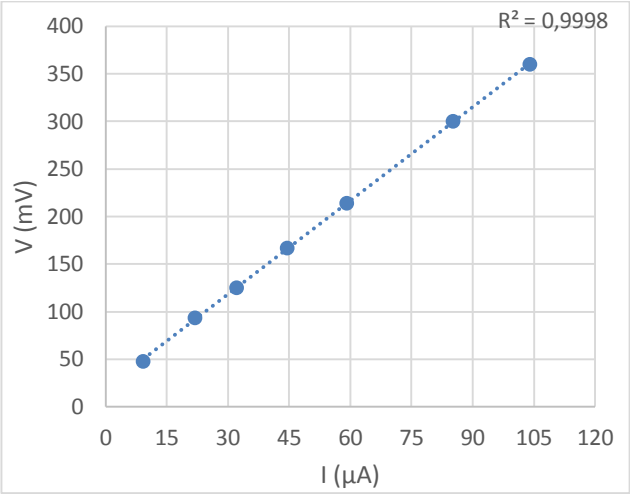

FIG. 8 V(I) of SnO disc 1, the slope is the resistance $R_{12,34}$=3279,4 Ω.

Due to the dispersion of the results of the carrier concentration an exact value for mobility could not be given but the value oscillates between 10^2 and 10^3 $cm^2 \cdot V^{-1} \cdot s^{-1}$, which is also of the order of the values of standard semiconductors like silicon or gallium arsenide.

The results obtained for SnO are in good agreement with the expected order of magnitude. However, they are much more imprecise than those obtained for the reference thin film reported in table (1), which are very accurate, and it is probably due to the geometry and thickness of the films. In the thin-film materials, the layers are deposited on glass substrate and their thicknesses are in the order of 10^{-7}m, while the SnO disc is polycrystalline SnO with no substrate and its thickness is way larger, about 10^{-3} m. This difference of thickness derives in a lower Hall's effect due to equation (6).

So the Hall's voltage is inversely proportional to the material thickness, and a change of four magnitude orders is big enough to reach the instrumental limitation making the results very inaccurate. Furthermore, I was constrained to use low magnetic fields due to the limitation in materials availability and time.

Another difference between these two conformations is the shape. The thin-film proving materials are square shapes and the SnO is a disc. The design of the holder and contacts distribution was thought for square distributions in the first place because it was expected to obtained thin films of SnO on glass substrates. The problem of the solubility arrived after the construction of the instrument and the distribution of contacts were not symmetric for circulars areas. This asymmetry derived in a bad Hall's effect determination due to the paths of the carriers are not equivalent in the 13 direction to the 24 direction (vertical and horizontal). This problem could be solved with changing the redistribution of the contacts, but this effect is minor than the thickness effect.

IV. CONCLUSIONS

I can conclude that the SnO powder was successfully synthesized, despite of do not achieving the development of the SnO ink due to its high chemical complexity. Moreover we can control the formation of SnO_2 by heating over 576ªC the powder, with its high potential in the development of thin film transistors. I have confirmed the *p*-type behaviour of the obtained SnO semiconductor with a low carrier concentration around 10^{12} cm^{-3} but with high mobility of the majoritarian carriers. Both the obtained carrier concentration and mobilities are similar to those of principal semiconductors like silicon or GaAs. This work stablishes the chemical route for achieving p-type SnO and confirms its good electrical properties, so it can be used as starting point for the developing of a SnO ink which can open the possibilities for a p-n complementary printed logic.

Acknowledgments

I would like to thanks Anna Vilà and Alberto Gomez for their help and support in the developing of this work and all my frieds and family that were an important moral support.

[1] J. Um, B.-M. Roh, S. Kim and S. E. Kim, "Effect of radio frequency power on the propierties of p-type SnO deposited via sputtering," *Materials Science in Semiconductor Processing*, no. 16, pp. 1679-1683, 2013.

[2] H. Yabuta, N. Kaji, R. Hayashi, H. Kumomi, K. Nomura, T. Kamiya, M. Hirano and H. Hosono, «Sputtering formation of p-type SnO thin-film transistors on glass toward oxide complimentary circuits,» *Applied Physics Letters*, nº 97, 2010.

[3] J. Caraveo-Frescas and H. Alshreef, «Transparent p-tpe SnO nanowires with unprecedented hole mobilit among oxide semiconductors,» *Applied Physics Letters*, nº 103, 2013.

[4] S. Yu, W. Zhang, L. Li, D. Xu, H. Dong and Y. Jin, "Fabrication of p-type SnO2 films via pulsed laser deposition method by using Sb as dopant," *Applied Surface Science*, no. 286, pp. 417-420, 2013.

[5] S. Majumdar, S. Chakraborty, P. Sujatha Devi and A. Sen, «Room temperature synthesis of nanocrystalline SnO through sonochemical route,» *Materials Letters*, nº 62, pp. 1249-1251, 2008.

[6] Y. Liang, H. Zheng and B. Fang, «Synthesis and characterization of SnO with controlled flowerlike microstructures,» *Materials Letters*, nº 108, pp. 235-238, 2013.

[7] E. Widberg y A. Frederick Holleman, Inorganic Chemestry, Elsevier, 2001.